Journal of Medical Systems (2019) 43: 23
https://doi.org/10.1007/s10916-018-1140-1

PATIENT FACING SYSTEMS

Infrared Thermal Imaging for Diabetes Detection and Measurement

A. Selvarani [1] · G. R. Suresh [1]

Received: 31 October 2018 / Accepted: 12 December 2018 / Published online: 2 January 2019

Abstract

The diabetes mellititus (type 1) condition occur when the beta cell destroy partially due to autoimmune process. The beta cells produce insulin with respect to blood glucose level. The insulin hormone regulates blood glucose in body. The blood glucose increases in body when insulin secretion is low from pancreas, termed as Diabetes mellititus. The Diabetes mellititus causes infection, pain in mouth. The regions in mouth affected by diabetes mellititius include gums, teeth, jaw and tongue. The glucose level increases in saliva which grows harmful bacteria. The bacteria in combination with plaque cause bad breath, gum disease and coating on tongue. The coating and sugar level in tongue alters the temperature of tongue. In this paper we propose to analyze tongue thermal image to diagnose diabetes at early stage.

Keywords Tongue · Diabetes mellititus · Plaque · Glycemic index

Introduction

Traditionally physicians use body temperature as a metric to diagnose different diseases. The body temperature varies in correlation to disease. The temperature measures with devices such as thermistors, thermocouples and thermopiles. The sensors characteristics such as size and sensitivity make hard to implement with moving organs. The sensor requires making contact with organs to measure temperature. Infrared thermal cameras provide a non invasive means to detect temperature of organs for metabolic disorder and disease diagnosis.

The Diabetes Mellitus (DM) and Non-proliferative Diabetic Retinopathy diagnosis (NPDR) is detect through Non-invasive method, as well as tongue images capture by using a non-invasive technique with image alteration, such as include colour, geometry and texture. A tongue having 12 shades, each colour represents the features of the tongue [1]. Two elements are chromatic & textural calculate and remove from tongue images via digital image processing method. Bayesian networks are appointing to the relationship between diseases and the quantitative features [2]. Diabetic Retinopathy based on three groups removed from tongue images at the starting stage. Based on measurements, areas, ratios 13 characteristics extracted from tongue images. Computerized tongue inspection techniques used to address tongue diagnosis. Computerized tongue disease it's estimated the different features are preliminary processing, tongue diagnosis, tongue investigation, and traditional Chinese medicine, characteristic extraction [3].

Traditional Chinese Medicine is one of the essential methods in Tongue diagnosis. In clinical therapy, classical tongue disease pertained with found syndromes tongue abnormal aspect and illness. If the current diagnosis tendency combine, the lack of sufficient survey, and high volume work have been finishing on the automatic tongue diagnosis. In Automated Current Diagnosis structure, the authors study about the advantages, potential, and research gaps. The authors apply algorithms in tongue detection, current tendency and global essential health province to move to automated tongue detection structure. A low-power processor is applied which can execute signal processing change raw magnetic

This article is part of the Topical Collection on *Patient Facing Systems*

✉ A. Selvarani
aselvaraniresreach@gmail.com

G. R. Suresh
sureshgr@rediffmail.com

[1] Department of Electronics and Communication Engineering, Sathyabama Institute of Science and Technology, Jeppiaar Nagar, Rajiv Gandhi Road, Chennai, India

sensor to user commands on the headset, instead of sending all raw data to a PC or smartphone. The method diminishes the transmitter power increases the battery life. Notified user problems one command each 20 ms, the advanced local processor minimises the information that needs be wirelessly transferred by using the factor of 64, from 9.6 to 0.15 kb/s. This method has three main blocks: serial fringe interface transport for getting raw information from the magnetic sensors, external magnetic field to attenuate from the natural magnetic signal, and a machine learning classifier for command diagnosis [4].

The method investigated dynamic infrared thermal images & blood perfusion between the relationship. The 62 anaemia victims & 70 authority subjects were calculated are different locations the rates of the blood perfusion. All groups thermal images is recorded, after 16 s mouth opened. Blood perfusion results showed at rates different sites on the tongues; anaemia victims were minimum than control sites. After mouth opened, tongue temperature was minimised in anaemia victims than control subjects rapidly. When the tongue was developed heat transfer contrivance, temporary heat transfer by using tongue temperature, and tongue temperature of anaemia victims & control subjects was calculated [5]. In self-diagnosis, visual examination of human tongue renders a compact, quick and non invasive solution. Analysis of the texture, geometrical shape and the color of the tongue gives a pathological information of the human body. The tongue color may indicate Parkinson's disease, nutritional deficiency, cancer and the texture of the tongue can indicate diabetes, down syndrome. Using a computer based diagnosis that utilizes digital image processing methods provides a way to identify these types of diseases. These digital image processing methods include acquisition of tongue image, image preprocessing and image classification for diagnosis. The statisitical distribution of human tongue's in-depth analysis provides a color space for feature extraction. The color of the tongue in is the color space that is the range of the colors consisting of colorcenters of categories of colors of 12 tongue. Analysing the typical image features of the tongue is through the color range of the tongue. The CIE chromacity diagram gives the range of color of the tongue. The chromacitydiagram uses a color range boundary descriptor based on a one class support vector machine algorithm [6]. The texture of the tongue image in show a difference by the distributions of the colorof the several typical features of the tongue such as red points and petechial points. Obtaining these tongue features establish a relationship between the color space of the tongue and distribution of the color of different tongue feature.

Tongue's interaction with the hard palate is the main process during speech and swallowing process. Due to the range of motion and tongue weaknesses, cerebrovascular diseases such as speech disorders and swallowing disorders occurs. So to identify the tongue motion range and tongue weakness, the solution is measuring the pressure of the tongue. So a new method called implantable intraoral device to measure the pressure of the tongue. This implantable intraoral device measures the pressure of the tongue on the hard palate inside the oral cavity directly and the transmitting the data through a wireless link [7].

For medical applications an in-depth systematic color analysis system for tongue analysis is suggested. Using the range of color of tongue in extracting the tongue foreground pixels and assigning to one of the 12 colors representing the color range of tongue. For the entire image, forming a tongue color feature vector is through calculating each color ratio [8].

The tongue images by a smartphone camera show a difference in color due to different lightning conditions and this impacts the diagnosis when using the white tongue appearance to identify the health conditions. Hence a capturing a pair of tongue images with and without flash and showing the color variation between the pair of tongue images provides a way to determine the lightning condition based on support vector machine. For three kinds of common lights that is fluorescent, incandescent and halogen, the color correction matrices are already trained by utilizing a color checker –based method and uses the already trained matrix to remove the color distortion effect [9]. In traditional Chinese medicine tongue use as diagnostic tool to determine therapeutic efficacy and peptic ulcer diseases (PUD). The tongue colour changes from light.

Red to dark red coated with yellow slimy fur with blood colouration in sublingual veins in Helicobacter pylori (HP) infected patients. In PUD patients the tongue fur changes to yellow [10]. Gastrointestinal affected peoples tongue color, coating thickness and temperature change with level of disorder [11]. The tongue forms blood stasis in type 2 diabetes patients. The blood stasis on tongue expose as petechiae, bluish colored tongue, sublingual collateral vessels. The petechiae and bluish tongue undergoes changes with level of lipoprotein and blood triglyceride [12]. Diabetic Patients undergoing chemotherapy for brain tumours develop black hair tongue (BHT) with in 10 day period other patients took more than 100 days to develop BHT [13].

In this paper, tongue heat variations analyse with dyadic wavelet transform algorithm (DyWT) for diabetes detection. The heat expelled from tongue varies for diabetic person and normal person. The thermal image of tongue acquires and process to evaluate heat regions in tongue. The region detection provides means for diabetes diagnosis at early stage. The study conducts only on type 1 diabetic person.

Materials and methods

The thermal image and color image of diabetic tongue acquire with fluke infrared thermal camera. The thermal camera measures temperature between −10°c to +250°c and has infrared spectral band between 6.5um and 14um. The camera creates thermal images with field view 20 × 20 degree. The acquired thermal image of tongue process with dyadic wavelet transform and delta segmentation to detect temperature distribution of tongue. The tongue thermal image processing workflow of proposed methodology is shown in Fig. 1.

The participants involved in study were type 1 diabetic patient's and normal person between the age group of 35 to 45 years. The initial thermal image of tongue was acquired in the morning before food intake. After thermal image acquisition, both the group were given normal breakfast comprising of idli and sambar. The thermal image was acquired after one and a half hour of food intake. The thermal images process with stationary wavelet transform filter.

Stationary wavelet transform filter

The stationary wavelet transform (SWT) filter apply on image to smoothen the image. SWT analyses transient, non-stationary phenomena with unit in time. The stationary wavelet transform (SWT) is derived through modifying fundamentals of discrete wavelet transform (DWT). The SWT is framed to get over the disadvantage of translation invariance in DWT. The translation invariance is achieved by performing up sampling and down sampling in the DWT output and apply filter over up sampling results with factor of $2^{(j-1)}$. SWT is the inherently repeating strategy which posses equal number of samples in both input and output of algorithm. Thus, the N level of decomposition generates the same N level of redundancy in wavelet coefficient. Figure 2 shows the flow of stationary wavelet transform with three level filter banks.

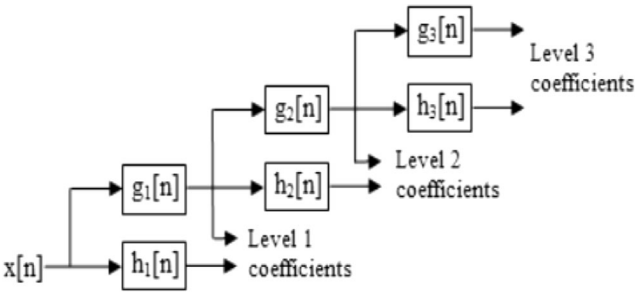

Fig. 2 SWT with 3 level filter

The input noisy image was applied to the SWT algorithm. The detailed sub bands generated from the output of SWT is applied to the soft thresholding method. The output image was framed from the approximated sub bands, other sub bands are represented as zero. The approximated sub band was applied to the inverse SWT algorithm to generated 2D set of array. The 2D array was applied to weighted median filter, which removes the noises in the input image and redundantly applied to the inverse SWT algorithm, which generates the denoised image through approximated threshold sub band. In SWT under sampling is replaced with redundancy, thus the filter tap is filled with zeros instead of decimalisation. The filtered image apply through median filter for robust mean value averaging leaving irrelevant pixels. The median filter better preserves edges by discarding irrelevant pixels in image.

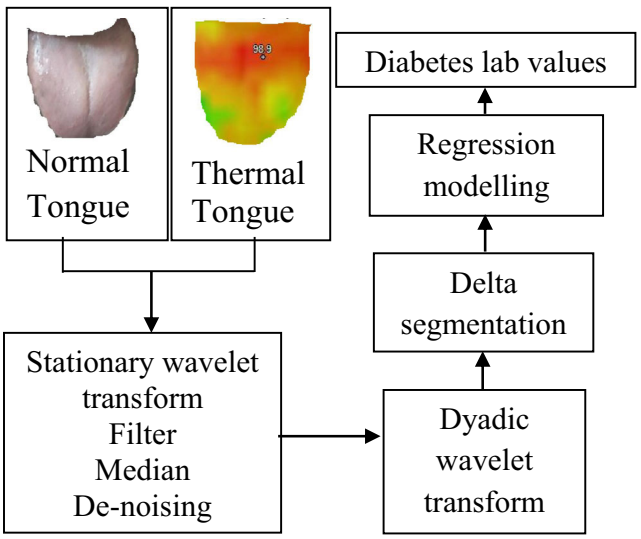

Fig. 1 Diabetic tongue Infrared thermography processing

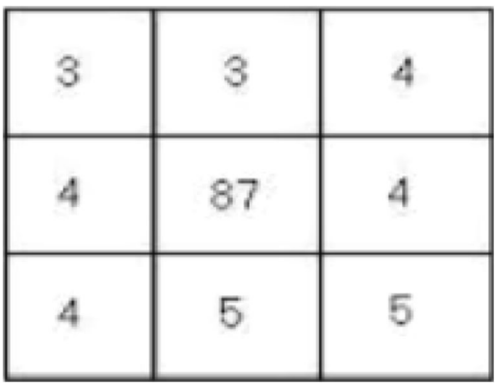

Fig. 3 Median Filter

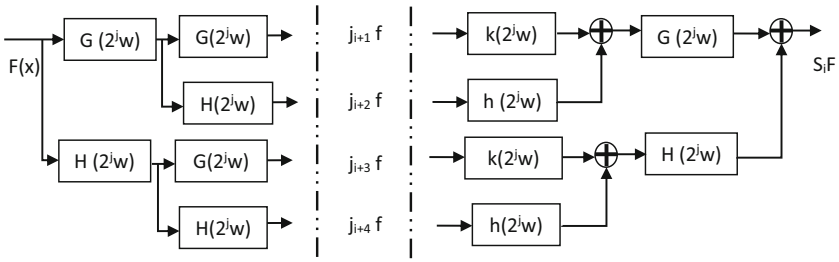

Fig. 4 Dyadic wavelet transform Filter bank

Median filter

Median filter is used to remove the pulsated noise in the input image. Each window is considered as a matrix and it assigns the medians of the matrix cells as an input value to the central cell of the given input matrix. Each window was selected and the pixel values of the window was sorted. The median was calculated from pixel value. The calculated median was compared with other medians of matrix with similar window size and the central cell is replaced with the processed median value. Figure 3 represent a window applied to the median filter were the sorted values are 3, 3, 4, 4, 4, 4, 5, 5, 87 and the median value of this window is 4.

Centre weighted median filter

The centre weighted median filter considers the middle cell value of the window. It checks the condition that the centre value satisfies, it is the largest value than other cell values or it is the smallest value than the other cell values. If the condition satisfies, the window is considered as corrupted window. The centre value is recalculated with other cell values and corrupted middle cell value is replaced with the calculated value. The weight was applied to the centre value, the other pixel values are sorted in ascending order, and the median of the window is calculated. This method is introduced to overcome the trade off in traditional median filter in managing noise suppression and detail maintenance. The filter fails to provide noise free image while preserving image quality. To overcome the above image process with SWT de-noising.

Image de-noising

The ambient noise in surrounding affects thermal image during acquisition. The noise in high and low depths of thermal image remove by convolution operators as shown below.

$$s_L = s_0 \cdot B_0 \cdot B_0^{'} \cdot \ldots \cdot B_{L-1} \cdot B_{L-1}^{'} \cdot B_L \cdot B_L^{'}$$
$$H_L = s_0 \cdot B_0 \cdot B_0^{'} \cdot \ldots \cdot B_{L-1} \cdot B_{L-1}^{'} \cdot A_L \cdot B_L^{'}$$
$$V_L = s_0 \cdot B_0 \cdot B_0^{'} \cdot \ldots \cdot B_{L-1} \cdot B_{L-1}^{'} \cdot B_L \cdot A_L^{'}$$
$$D_L = s_0 \cdot B_0 \cdot B_0^{'} \cdot \ldots \cdot B_{L-1} \cdot B_{L-1}^{'} \cdot A_L \cdot A_L^{'}$$

The noise free image process with Dyadic wavelet transform for thermal region edge enhancement. The mutiresolution and wavelet dilation features in DyWT produce better edges compared to conventional wavelets. The DyWT use mother wavelet to form dilation functions for edge detection. The dyadic wavelet transform construct with directional wavelets. The directional wavelets enable orientation filtering. The filtering projects blurred edges in region of

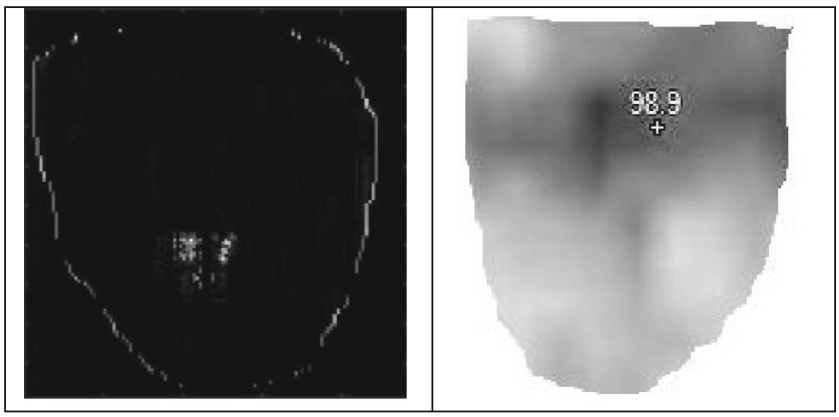

Fig. 5 Comparison of tongue thermal image processing with dyadic transform and wavelet transform

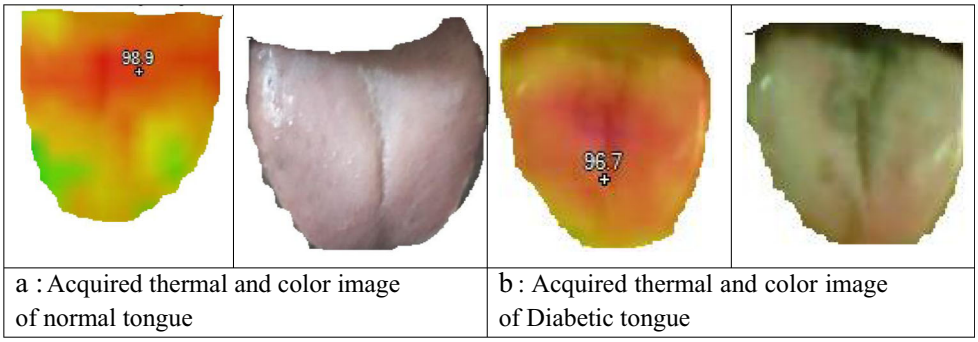

a : Acquired thermal and color image of normal tongue

b : Acquired thermal and color image of Diabetic tongue

Fig. 6 **a** Acquired thermal and color image of normal tongue. **b** Acquired thermal and color image of Diabetic tongue

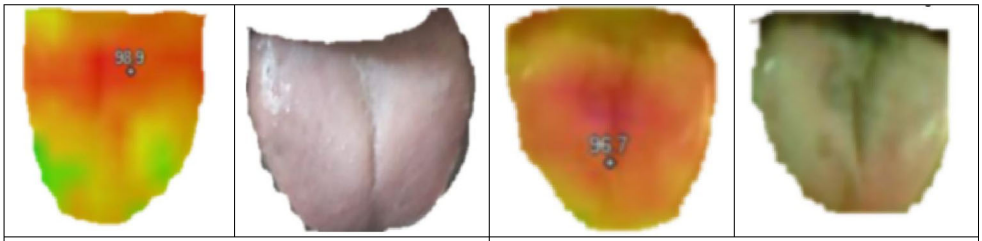

a : Bilinear filtering of normal tongue

b : Bilinear filtering of diabetic tongue

Fig. 7 **a** Bilinear filtering of normal tongue. **b** Bilinear filtering of diabetic tongue

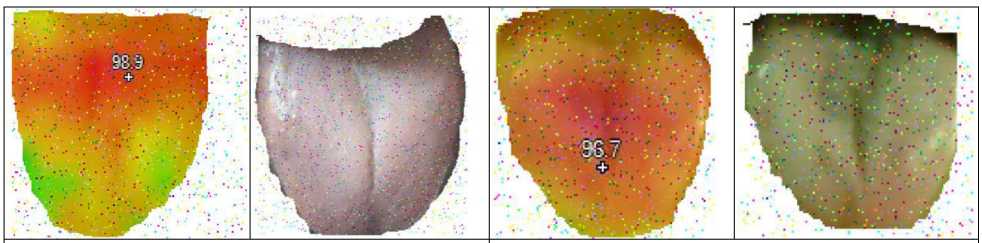

a : Median filtered normal tongue

b : Median filtered diabetic tongue

Fig. 8 **a** Median filtered normal tongue. **b** Median filtered diabetic tongue

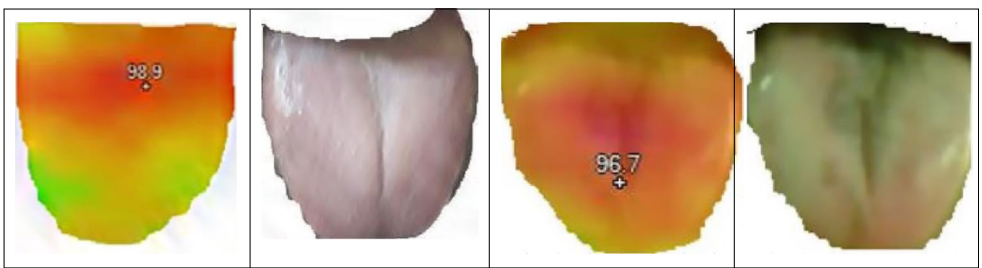

a : Normal tongue De-noised image

b : Diabetic tongue De-noised image

Fig. 9 **a** Normal tongue De-noised image. **b** Diabetic tongue De-noised image

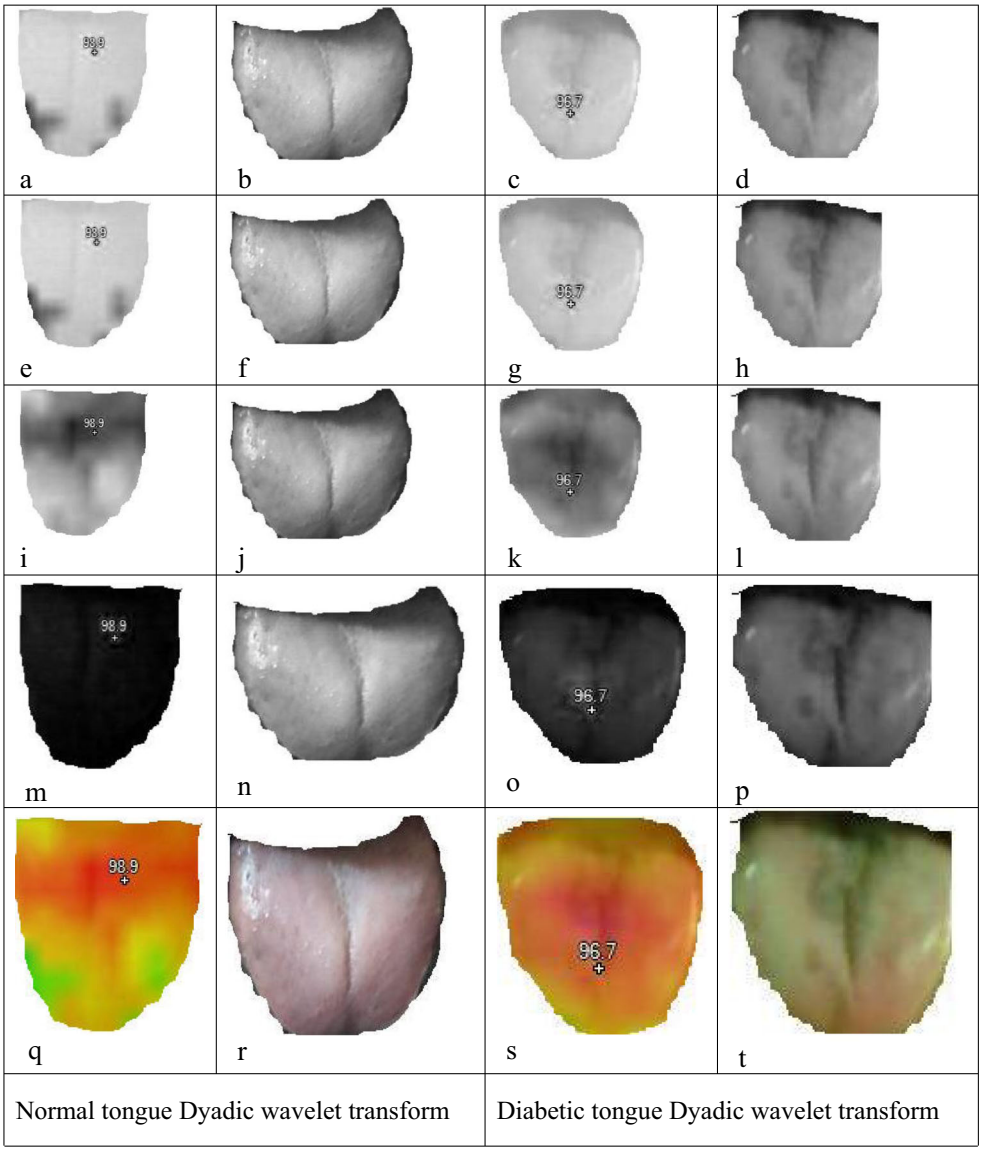

Fig. 10 Dyadic wavelet transform of normal and diabetic tongue

interest. However, wavelet transform produce discontinuity in blurred region of interest.

Dyadic wavelet transform

The dyadic wavelet transform represent by function f(x) with 2^k scales. The x position relatively changes with f and ψ convolution. The dyadic wavelet function represent by

$$W_{2^k} f(x) = f(x) * \psi_{2^k}(x)$$

The product of f and g is given by

$$f(x) * g(x) = \int_{-\infty}^{\infty} f(u) g(x-u) du$$

And $\psi_{2^k}(x) - \frac{1}{\sigma}\psi\left(\frac{1}{\sigma}\right)\Big|_{\sigma=2^k}$.

Which are the dilation factors of mother wavelet $\psi(x)$.

The input image f(x) represent in its corresponding wavelet form as

$$f(x) = \sum_{k=-\infty}^{\infty} W_{2^k} f(x) * X_{2^k}(x) = \sum_{k=-\infty}^{\infty} f(x) * \psi_{2^k}(x) * X_{2^k}(x)$$

Provided the wavelets $X(x)$and $\psi(x)$ satisfies the condition

$$\forall\omega,\ \sum_{k=-\infty}^{\infty} \hat{\psi}\left(2^k\omega\right)\hat{X}\left(2^k\omega\right) = 1$$

Where $X(x)$ and $\psi(x)$ Fourier transforms given by $\hat{X}(\omega)$ and $\hat{\psi}(\omega)$ respectively.

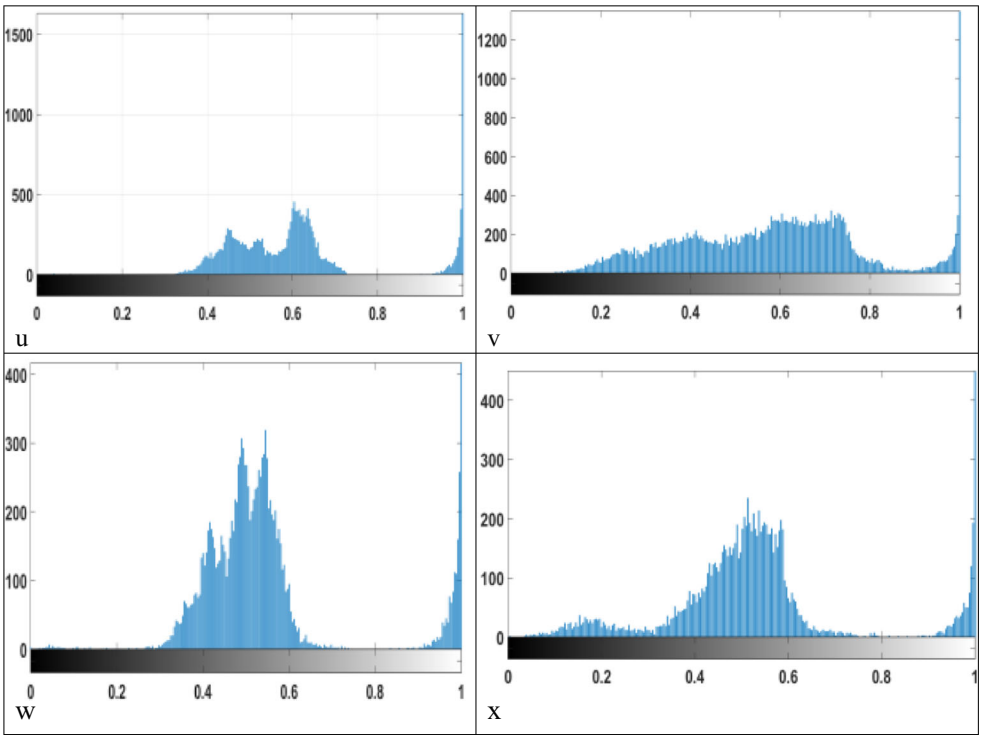

Fig. 10 continued.

The dyadic wavelets form with dyadic grid scaling functions represent by

$$\psi_{m,n}(t) = \frac{1}{\sqrt{\sigma_0^m}}\psi\left(\frac{t - n\tau_0\sigma_0^m}{\sigma_0^m}\right)$$

Where $\tau_0^- = 1$ and $\sigma_0 = 2^-$ which yields the equation

$$\psi_{m,n}(t) = \frac{1}{\sqrt{2^m}}\psi\left(\frac{t - 2^m}{2^m}\right)$$

Or in compact terms

$$\psi_{m,n}(t) = 2\frac{-m}{2}\psi(2^{-m}t - n)$$

The dyadic and inverse dyadic filter bank represent as shown in Fig. 4.

Delta e-colour segmentation

The dyadic wavelet transformed image shows the colour distribution in image and the covered region. The dyadic wavelet transform projects edges without discontinuity compared to conventional wavelet as shown in Fig. 5. The change in colour level and pixel distribution further segment and enhance with delta colour segmentation. In delta e colour segmentation the thermal image convert to lab colour space where the region of interest is selected. The selected region comprises of pixel for which the delta e colour calculate for each pixel in region. The enhanced pixel shows the thermal activity region of tongue in acquired image.

Results & discussion

The thermal and colour image of normal and diabetic tongue with fluke infrared thermal camera is shows in Fig. 6a and b. The acquired thermal images comprises of noise, reducing signal to noise ratio and thermal image contrast. The noise in thermal image occur due to signal processing circuit in thermal camera. The noise and surrounding environment varies pixel response in acquired thermal image. The noise in thermal image removes with bilinear filter which blurs the image as shown in Fig. 7a and b. The image blurs due to high signal to noise ratio in infrared thermal image. The median filter apply on image to sharpen and increase contrast of thermal image as shown in Fig. 8a and b. The salt and pepper noise in image removes with image de-noising as shown in Fig. 9a and b. The de-noised image process with dyadic wavelet transform as shown in Fig. 10.

In Dyadic Wavelet Transform (DyWT) the de-noised thermal image converts to R,G,B channel images. The individual R,G,B channel images process with dyadic

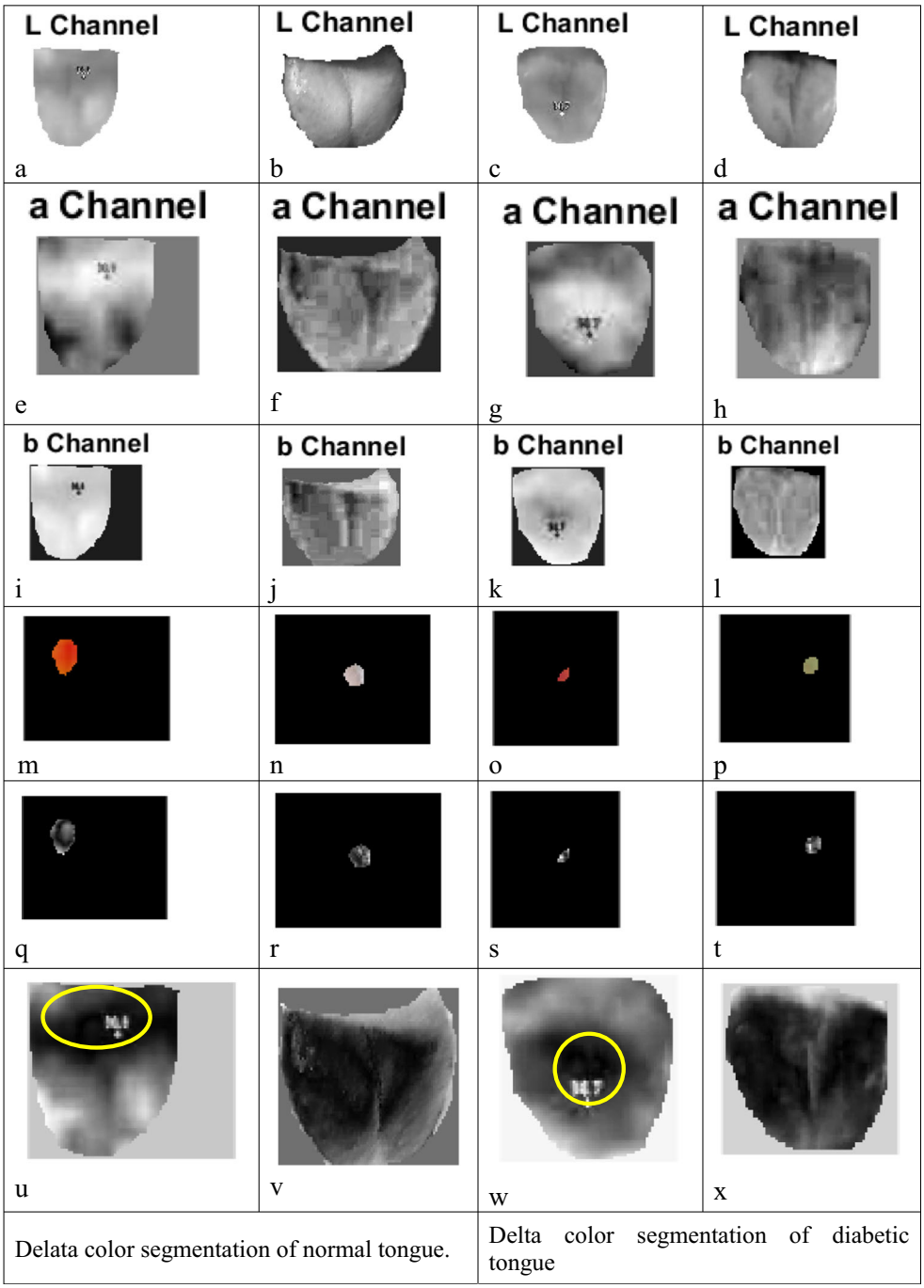

Fig. 11 Delta colour segmentation of normal and diabetic tongue

wavelet transform to project low thermal regions in tongue as shown in Fig. 10a, e for normal tongue and 10c, g for diabetic tongue. The high thermal active region for normal tongue is show in Fig. 10i, m and for diabetic tongue shown in Fig. 10k and o. The R, G, B channels for normal and diabetic tongue combine to form corresponding thermal and color image as in Fig. 10q, r, s and t and the corresponding histogram is shown in Fig. 10u to x.

The edge improved dyadic thermal image process with delta colour segmentation. In delta colour segmentation the grey scale image process in l, a -and b channels. The channels show thermal active region as grey level 1 and low thermal active region as grey level 0 for normal tongue in Fig. 11a, e, i and for diabetic tongue shows in Fig. 11c, g and k. The region of interest select with improved thermal activity select as in Fig. 11m and o for normal and diabetic tongue. From the

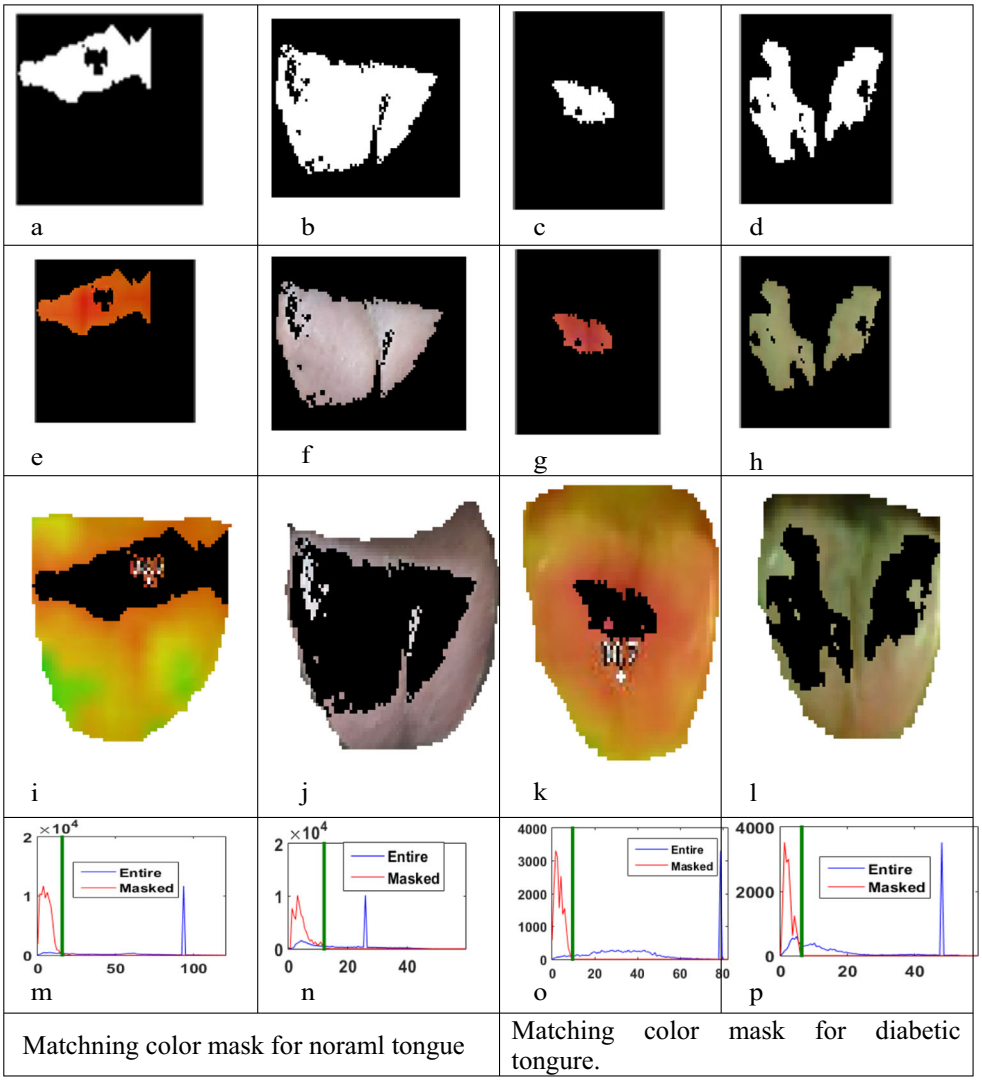

Fig. 12 Matching colour mask for normal and diabetic tongue

Fig. 11q and s it is observed that the thermal activity is reduced. The reduced thermal activity of tongue is highlighted in yellow colour in Fig. 11u and w. The thermal activity in tongue limits to only the centre region of tongue in diabetic patients whereas the thermal activity of normal person is spread over the entire tongue region is shown in grey level 0 and grey level 1 in Fig. 11u, v, w and x.

The tongue thermal distribution and adjoining pixels with similar pixels are clustered as shown in Fig. 12a and c. Comparing Fig. 12e and g the tongue temperature of diabetic patient is more compared to that of normal person. The tongue temperature distribution of normal person is high in medial sulcus and low in fungiform papilla as in Fig. 12i. The temperature distribution of diabetic tongue is uniform over the entire tongue region with minimal variations as in Fig. 12k and validate with histogram in Fig. 12m and o.

The thermal tongue image parameter for normal and diabetic person is tabulated in Table 1. The mean value of thermal

Table 1 Statistical analysis for normal and diabetic person tongue thermal image

Parameter	Normal person (Thermal image)		Diabetic person (Thermal image)	
	Before food	After food	Before food	After food
Mean	120.5058	126.258	112.595	187.34
Entropy	7.3405	12.5412	15.2485	18.264
Standard deviation	43.6353	35.29	58.264	46.54

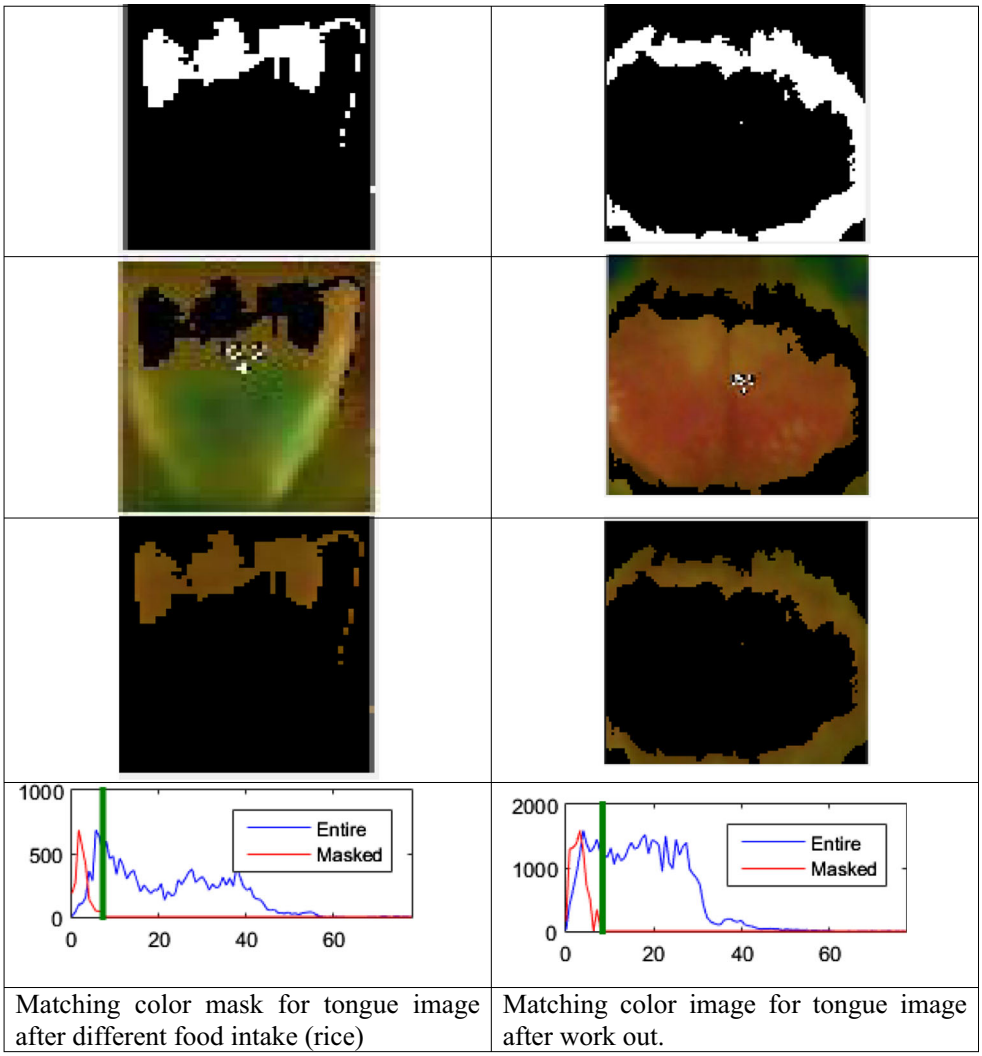

Matching color mask for tongue image after different food intake (rice)

Matching color image for tongue image after work out.

Fig. 13 Tongue thermal image comparison for rice food intake and tongue thermal activity after workout

image increases for normal and diabetic before and after food intake. Similarly, the thermal image standard deviation decreases afterfood intake for both category person. The regression model generate based on mean and standard deviation parameters. The Fig. 13 shows the comparative analysis of tongue thermal image for different food intake (rice) for diabetic person and to evaluate tongue thermal activity after half an hour jogging. The analysis shows reduced tongue thermal region for diabetic person. The tongue thermal activity for normal person is higher with respect to Figs. 12i and 13.

Regression modelling

The straight line of linear regression modelling is represented by

$$Y = a0 + a1\,X$$

Where ao is the intercept for glucose level and a1 is the slope.

The linear regression equation for diabetic person after food intake is given by

$$Y = 147.3 - 0.0116x$$

Where X is the mean values of diabetic tongue thermal image and Y is the glaucometer values.

Conclusion

In this paper, the thermal image of tongue acquire with thermal camera. The thermal image of tongue analyse for preclinical diabetes diagnosis. The potential of proposed methodology validate by acquiring tongue thermal image of 25 people from age group 30-35. The tongue thermal image of diabetic

and normal tongue process with bilinear filter to remove noise. The noise free image sharpen with median filter to project edges in thermal image. The Dywt (Dyadic wavelet transform) apply to map thermal active region in tongue. Comparative analysis of diabetic and normal tongue shows increased thermal active region for normal tongue before and after food intake.

Compliance with ethical standards

Conflict of Interest None.

Human and animal rights This article does not contain any studies with human participants or animals performed by any of the authors.

References

1. D. Zhang, H. Zhang, and B. Zhang, *Tongue Image Analysis*. 2017.
2. Pang, B., Zhang, D., Li, N., and Wang, K., Computerized tongue diagnosis based on Bayesian networks. IEEE Trans. Biomed. Eng. 51(10):1803–1810, 2004.
3. Tania, M. H., Lwin, K., and Hossain, M. A., Advances in automated tongue diagnosis techniques. *Integr. Med. Res.*, 2018.
4. Jafari, A., Buswell, N., Ghovanloo, M., and Mohsenin, T., A Low-Power Wearable Stand-Alone Tongue Drive System for People with Severe Disabilities. IEEE Trans. Biomed. Circuits Syst. 12(1):58–67, 2018.
5. Xie, H., and Zhang, Y., Relationship between dynamic infrared thermal images and blood perfusion rate of the tongue in anaemia patients. Infrared Phys. Technol. 89:27–34, 2018.
6. Wang, X., Zhang, B., Yang, Z., Wang, H., and Zhang, D., Statistical analysis of tongue images for feature extraction and diagnostics. IEEE Trans. Image Process. 22(12):5336–5347, 2013.
7. Borghetti, M., and Serpelloni, M., Measuring inside your mouth! Measurement approaches, design considerations, and one example for tongue pressure monitoring. IEEE Instrum. Meas. Mag. 19(5): 41–48, 2016.
8. Zhang, B., Wang, X., You, J., and Zhang, D., Tongue color analysis for medical application. *Evidence-Based Complement. Altern. Med.*, 2013, 2013.
9. Hu, M. C., *et al.*, Automated tongue diagnosis on the smartphone and its applications. *Comput. Methods Programs Biomed.* 0:1–14, 2018.
10. Wang, H.-H., Pan, C.-H., Wu, P.-P., Luo, S.-F., Lin, H.-J., and Wu, C.-H., Alteration of the Tongue Manifestation Reflects Clinical Outcomes of Peptic Ulcer Disease. J. Altern. Complement. Med. 18(11):1038–1044, 2012.
11. Wu, T. C. et al., Tongue diagnosis indices for upper gastrointestinal disorders: Protocol for a cross-sectional, case-controlled observational study. Med. (United States) 97(2):3, 2018.
12. Hsu, P. C., Huang, Y. C., Chiang, J. Y., Chang, H. H., Liao, P. Y., and Lo, L. C., The association between arterial stiffness and tongue manifestations of blood stasis in patients with type 2 diabetes. *BMC Complement. Altern. Med.*, vol. 16(1), 2016.
13. Yamagishi, Y. et al., Black hairy tongue after chemotherapy for malignant brain tumors. Acta Neurochir. 159(1):169–172, 2017.